

Roles of Hydrogen Bonding and the Hard Core of Water on Hydrophobic Hydration

Mitsunori Ikeguchi,* Seishi Shimizu, Shugo Nakamura, and Kentaro Shimizu

Department of Biotechnology, The University of Tokyo, Yayoi 1-1-1, Bunkyo-ku, Tokyo 113-8657, Japan

Received: November 14, 1997; In Final Form: April 8, 1998

The roles of hydrogen bonding and the hard core of water on hydrophobic hydration are clarified using Monte Carlo simulation and the test particle method to compare the cavity formation in water with that in a Lennard-Jones (LJ) fluid with the same molecular size and density. Similarities and differences in the cavity formation in the two fluids are examined in terms of the free energy, the energy change, and the change in the coordination number upon cavity formation. The free energy of cavity formation *at a given density* and the decrease in the coordination number around cavities in water are similar to those in the LJ fluid. These similarities are due to geometrical restriction of the hard core of molecules. The effect of the hydrogen bonding of water can be seen in the coordination-number dependence of the average energy of one molecule, regardless of whether water is in bulk or in the hydration shell. The temperature dependence of the correlation between the coordination number and energy can explain both the temperature dependence of hydrophobic enthalpy in the thermodynamic level and that of molecular energy changes near cavities in the molecular level. We conclude that combining the water-specific coordination-number dependence of energy (the hydrogen-bonding effect) with the decreased coordination number around hydrophobic groups (the hard-core effect) explains the special characteristics of hydrophobic hydration, such as iceberg formation, the entropy decrease at room temperature, and the large positive heat capacity change.

1. Introduction

Hydrophobic effects play a very important role in various molecular phenomena such as protein folding, lipid membrane formation, and molecular recognition. Elucidating the molecular mechanism of hydrophobic hydration will contribute to the understanding of such phenomena. Furthermore, the understanding of the mechanism itself is also interesting and a challenging issue.

Solubility data of nonpolar molecules in water have been widely used as an indicator of hydrophobic effects.^{1–8} The “pseudo chemical potential” proposed by Ben-Naim provides the theoretical background which bridges the experimental data and the statistical mechanics.^{1,2,9–11} Solubility data have been parametrized in various ways, such as coefficients of solvent-accessible surface area of molecules, and have been widely applied to estimation of hydrophobic effects of molecules.^{3–8}

The characteristics of thermodynamics of hydrophobic hydration are summarized as follows:¹² (1) There is a large positive solvation free energy upon the solution of hydrophobic molecules. (2) At room temperature, entropy dominates the free energy. At high temperatures (110–200 °C), instead of entropy, enthalpy dominates the free energy. (3) There is a large positive heat capacity change of solvation.

To explain these characteristics, numerous theories and hypotheses concerning the molecular mechanism of hydrophobic hydration have been proposed over the past several decades. The most widely accepted explanation is “iceberg formation”.¹³ The decrease of the entropy upon hydrophobic solution at room temperature is explained as the formation of an iceberg around nonpolar groups. The heat-capacity increment is explained as the iceberg melting. There is experimental evidence of strengthening of hydrogen bonds around hydrophobic solutes.¹⁴ Re-

cently, using the random network model and Monte Carlo simulation, Madan and Sharp^{15,16} observed icelike hydrogen bonds of water around nonpolar groups.

There is another point of view concerning the effect of the water structuring (such as the iceberg) on the hydrophobic effect.^{12,17,18} At high temperatures, the entropy change becomes small (or zero at the temperature at which the iceberg is considered to have melted). However, the free energy change is larger at high temperatures than at room temperature. Therefore, it was concluded that the water structuring does not strengthen the hydrophobic effect but weakens it, and that the main contribution to the hydrophobic effect comes from the breaking of the hydrogen bonds.

Both theories, iceberg formation and hydrogen-bond breakage, are based on the hydrogen bonding of water. However, there are studies that take another approach concerning the hydrophobic effect. In these studies, the hard core of water molecules is more important to the hydrophobic effect than the hydrogen bonding of water is. Pierotti^{19–21} showed that the scaled particle theory (SPT), which is a hard-sphere fluid theory, can be used to predict the hydrophobic solvation free energy. The theory only uses the molecular size, density, and pressure of water as inputs and does not explicitly include any special features of hydrogen bonding of water. The effect of hydrogen bonds of water is implicitly taken into account through the size and density of water. On the basis of the SPT, it was pointed out that the origin of the hydrophobic effect is the smallness of water.^{22,23} The importance of the hard-core overlap between solvent and solute was also pointed out using methods other than the SPT by Lee.²⁴ He divided a hydrophobic solvating process into subprocesses and, using Widom’s potential distribution theory, concluded that exclusion of the hard-core overlap between solvent and solute is most responsible for the hydrophobicity. Madan and Lee²⁵ calculated the free energy of cavity

* To whom correspondence should be addressed.

formation in water and simple Lennard-Jones (LJ) fluids, which have almost the same size and density as water, and they found that both free energy values are very similar.

The two approaches look very different: one is based on the hydrogen bonding of water, and the other is based on the hard core of water. A unified physical picture of hydrophobic hydration, which includes the essence of both types of theory, needs to be developed. Numerous computer simulations^{15,16,26–42} and integral equation studies^{43–52} have been done on hydrophobic effects. Such explicit water simulations and theories can give insights into such a unified picture. Pohorille and Pratt^{37,38} studied the cavity formation in various liquids including water and found that the cavity work predicted by the SPT is 20% below the numerical data of water. They concluded that the free volume of water is distributed in smaller packets because of a hydrogen-bonding network and that the hard-sphere liquid finds more ways to configure its free volume in order to make a cavity. However, they did not calculate how the hydrogen bonding of water is changed by cavity formation, and the role of the hydrogen bond remains unclear. Lazaridis and Paulaitis^{39,40} examined the hydrophobic entropy in terms of the molecular correlation function. They divided the hydrophobic entropy into translational and orientational entropy, but a detailed physical picture of the roles of the hard core and hydrogen bonds of water was not made clear. Matubayasi⁴¹ studied water geometry around hydrophobic solutes but did not study its relationship to the free energy or the heat capacity change. Madan and Sharp^{15,16} studied the relationship between water geometry and the heat capacity change using the random network model but did not consider the free energy of the hydrophobic solution in their paper.

In this paper, we propose a unified physical picture of the hydrophobic hydration based on both the hydrogen bonding of water and the hard-core effect. Cavity formation in the LJ fluid whose molecular size and density are the same as those of water is compared with cavity formation in water using the test particle method. Similarities and differences between the two fluids are examined in terms of the free energy of cavity formation and the energy change around cavities, and, then, how change in the water geometry around cavities causes the energy change is examined. Furthermore, to understand the mechanism of the heat capacity change caused by hydrophobic hydration, a simulation at high temperature was performed. A detailed picture of iceberg formation around hydrophobic solutes is clarified from these results.

2. Methods

The free energy upon cavity formation (ΔG) was calculated using the test particle procedure.^{53,54} First, a Monte Carlo simulation of the pure liquid was performed, and its configurations were recorded. Then, cavities were generated at random locations for each configuration and were tested as to whether they overlapped solvent molecules. From the probability of success of the insertions, the free energy of the cavity work was easily obtained using

$$\Delta G = -kT \ln \langle \exp[-\Delta U/kT] \rangle_0 \quad (1)$$

where k is the Boltzmann constant, T is the absolute temperature, and $\langle \rangle_0$ expresses the ensemble average using the distribution of solvent configurations *before* insertion of a solute. If one or more solvent molecules overlap the cavity, ΔU becomes infinitely large; otherwise, it is 0. Therefore, the term $\exp[-\Delta U/kT]$ is limited to either 0 or 1.

When spherical cavities are inserted, cavities with various radii can be simultaneously sampled. Let λ be $R_{\text{cavity}} + R_{\text{solvent}}$, where R_{cavity} and R_{solvent} are the radii of a cavity and a solvent molecule, respectively. Because any cavity whose λ is less than the distance to the closest molecule to a sampled point can be inserted, a histogram of the distance to the closest molecule gives the insertion probabilities of cavities with various radii. Then the free energy of the cavity work for various radii can be obtained. This method is similar to a method introduced by Pohorille and Pratt.³⁷ They used a three-dimensional grid to sample cavities, while we sampled them at random locations. The efficiency of both methods is almost equal.

The energy change ΔE upon cavity formation can be calculated from the pure liquid simulation by

$$\Delta E = \frac{\langle U e^{-\Delta U/kT} \rangle_0 - \langle U \rangle_0 \langle e^{-\Delta U/kT} \rangle_0}{\langle e^{-\Delta U/kT} \rangle_0} \quad (2)$$

where U denotes the potential energy of the pure liquid. If molecules outside a certain hydration shell are assumed to be energetically equivalent to bulk molecules, the energy change equals the following energy change in the shell around a cavity ΔE_{shell}

$$\Delta E_{\text{shell}} = \frac{\langle \langle \sum_{i \in \text{shell}} e_i \rangle e^{-\Delta U/kT} \rangle_0}{\langle e^{-\Delta U/kT} \rangle_0} - n_{\text{shell}} \langle e_i \rangle_0 \quad (3)$$

where $\sum_{i \in \text{shell}}$ denotes the summation for molecules within the shell and n_{shell} is the number of molecules within the hydration shell. e_i is the energy of the molecule i and is defined by

$$e_i = - \sum_{j \neq i}^1 u_{ij}(\mathbf{r}_i, \mathbf{r}_j) \quad (4)$$

where $u_{ij}(\mathbf{r}_i, \mathbf{r}_j)$ is the potential function between molecules i and j , and \mathbf{r}_i and \mathbf{r}_j are coordinates of molecules i and j , respectively. Of course, if one chooses a hydration shell that covers the overall system, eq 2 is exactly equivalent to eq 3. In this paper, the shell width for ΔE_{shell} was set to 2.8 Å to correspond to the first shell of water around cavities, because the statistical uncertainty of ΔE_{shell} becomes large if more than one water shell are included. For valid calculation of ΔE_{shell} when more shells are included, a longer simulation is needed. Previous studies, however, suggest that the first water shell contributes about 70% of the hydration-energy change.⁴¹ We believe that the energetics of the first water shell reasonably represent the characteristics of hydrophobic hydration as discussed in section 3.

All Monte Carlo simulations were done under the following conditions: A system of 216 TIP4P⁵⁶ water molecules and a system of 216 LJ particles were considered. A periodic boundary condition was applied. All simulations were done under a constant pressure of 1 atm. Parameters of the LJ potential were the same as those used by Pratt and Pohorille.³⁸ The parameters were set so that the mean particle–particle distance at 1 atm would be the same as the oxygen–oxygen distance of water. LJ interactions and electrostatic interactions were truncated at 8.5 Å. During each run, at least 4 million configurations were generated for equilibration, and 20 million configurations were generated as sampling configurations. To estimate the statistical uncertainty of the statistical values, we divided one sequential run into five subruns and obtained the minimum and maximum values for each run. Coordinates were recorded at every 2000 configurations. For isobaric sampling,

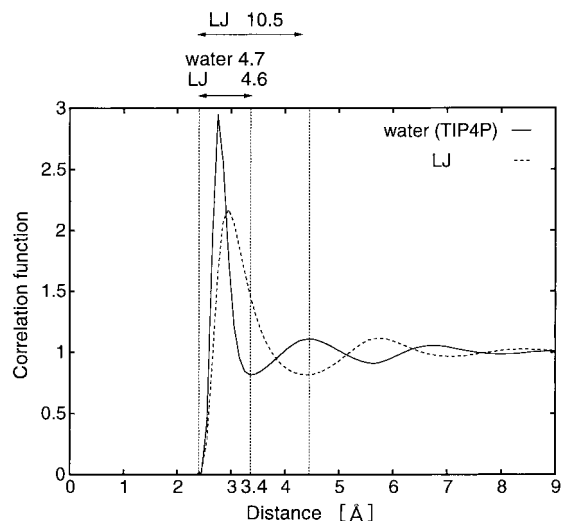


Figure 1. Correlation functions of water and the LJ fluid. 3.4 Å is the threshold distance for calculation of the coordination number. The numbers on top of this plot are the average coordination numbers of two liquids. For the LJ fluid, the number of neighboring molecules within the first minimum of the distribution function is also presented. (See text in detail.)

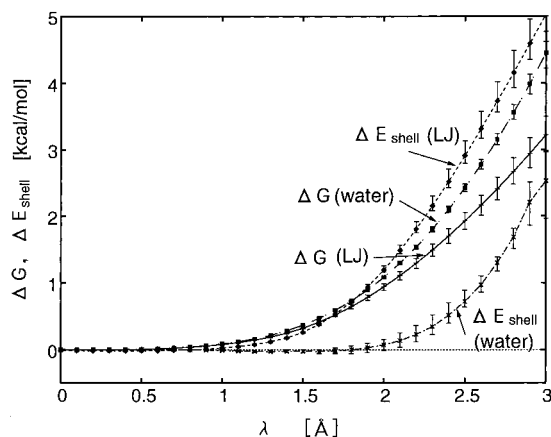


Figure 2. Free energy ΔG and energy change ΔE_{shell} in the hydration shell upon cavity formation in water and in the Lennard-Jones fluid at 300 K. λ is the sum of the radii of the cavity and solvent.

we attempted to scale the system volume at every 600 configurations.

3. Results and Discussion

3.1. Cavity Formation in Water and in the Lennard-Jones Fluid at 300 K. The free energy (ΔG) and ΔE_{shell} of inserting cavities with λ of 0–3.0 Å in water at 300 K were calculated. To analyze the role of the special liquid structure of water, ΔG and ΔE_{shell} of cavity formation in a simple LJ fluid, which did not have the special liquid structure (unlike water), were also calculated and compared with that in the case of water. Figure 1 displays the correlation functions of water and the LJ fluid. The exclusive distance 2.4 Å of the LJ fluid is observed to be the same as that of water. The correlation functions beyond 2.4 Å are different, which express the difference of the liquid structures such as the hydrogen-bonding network of water.

ΔG and ΔE_{shell} of cavity formation are shown in Figure 2. In water, ΔE_{shell} is much smaller than ΔG , and this corresponds to the large entropy decrease at room temperature in hydrophobic hydration. On the other hand, in the LJ fluid, ΔE_{shell} is larger than ΔG , which suggests that cavity formation in the LJ fluid is rather enthalpic. While ΔE_{shell} is very different between

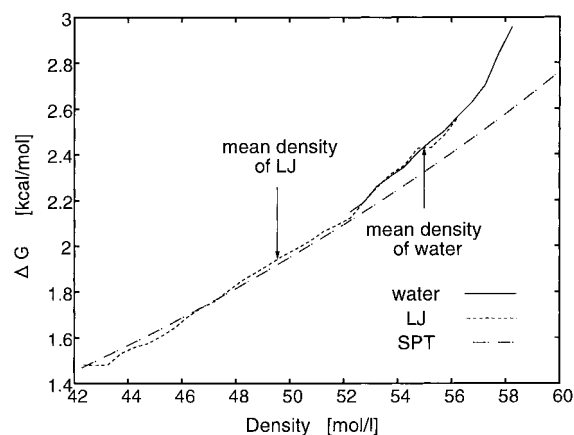


Figure 3. Free energy ΔG of cavity formation for various densities. Cavity formation in water (solid line) is compared with that in the Lennard-Jones fluid (dashed line). The result from the scaled particle theory (SPT) is also plotted.

water and the LJ fluid, ΔG in water is only slightly larger than in the LJ fluid. We attempted to clarify the difference between ΔG in water and in the LJ fluid in more detail. In Figure 3, ΔG of cavity formation with λ of 2.5 Å is plotted against the density of both fluids. Because the density of the system fluctuates in the isobaric Monte Carlo simulation, configurations with various densities around the mean value could be sampled. Both in water and in the LJ fluid, ΔG of cavity formation is the same for the densities 52–56 mol/L. The difference in ΔG of the two fluids in Figure 2 is due to the difference in the mean densities of the two fluids. Madan and Lee²⁵ also calculated the free energy of cavity formation in LJ fluids under constant volume and obtained a free energy close to that of water. However, they did not adjust the LJ parameter so that the density was comparable to water at 1 atm. The pressure of their system is suspected to have been high, and the $P\Delta V$ term would not be negligible in such a case. (See the comment in the ref 25). Because our simulation was performed under constant pressure and we used an LJ parameter so that the density is comparable to that of water at 1 atm, the $P\Delta V$ term is negligible. Pratt and Pohorille³⁸ adjusted the LJ parameters and did their simulation under a constant pressure, but they only compared the average free energy at 1 atm. Our analysis reveals the density dependence of the free energy of cavity formation.

The similarity of the free energy in water and the LJ fluid is thought to be related to the fact that the hydrophobic free energy can be predicted by the scaled particle theory (SPT).^{19–21} In Figure 3, ΔG as predicted by the SPT is also plotted. We set the solvent radius in the SPT as 1.35 Å, as Pierotti did. As pointed out by Pohorille and Pratt,³⁷ near the density of water (55 mol/L), ΔG of the SPT is lower than the numerical data for water. Considering that the LJ fluid has the same ΔG as water, the small ΔG of the SPT may be due to the difference between the hardness and softness of the potential function. In consequence, our results support the hypothesis that the hydrophobic free energy is mainly determined by the molecular size and density, and less by the special liquid structure of water. To understand the molecular mechanism that accounts for the similarity of the free energy and the difference in the ΔE_{shell} , it is very important to develop a total view of hydrophobic hydration, including both hard-core theories, such as the SPT, and hydrogen-bonding theories, such as iceberg formation.

3.2. The Coordination Number and the Energy Change upon Cavity Formation. To analyze the relationship between ΔE_{shell} and the geometrical change of the solvent in the vicinity

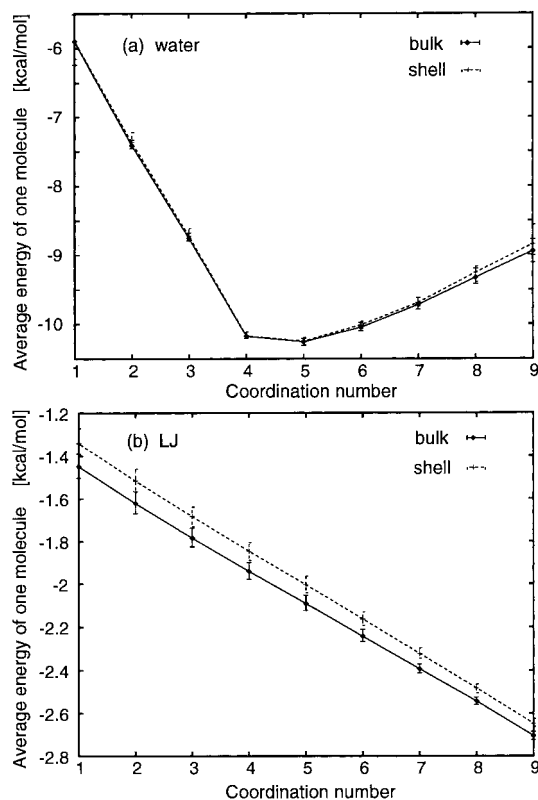


Figure 4. Average energy of one molecule against the coordination number for (a) water and (b) the Lennard-Jones fluid. The energies of the bulk molecules are compared with those of the shell molecules around a cavity with λ of 2.5 Å.

of cavities, the local density is more useful than the global density used in the above analysis of the free energy. The coordination number of water, which is defined as the number of neighboring molecules within 3.4 Å (the first minimum distance of the water–water correlation function (Figure 1)), is introduced as a measurement of the local density. To compare the LJ fluid with water in the same condition, the threshold distance of the coordination number of the LJ fluid is also set to 3.4 Å in this paper. Because 3.4 Å is not the minimum distance of the LJ–LJ correlation function (Figure 1), the LJ coordination number used in this paper is not the usual LJ coordination number. However, for convenience, we use the term “the coordination number” as a measurement of the local density of the LJ fluid in this paper.

The average energy of one molecule $e_{\text{ave}}(c_n)$ is plotted against the coordination number c_n in Figure 4. In the case of bulk water (Figure 4a), the average energy linearly decreases with the coordination numbers from 1 to 4 but increases from 5 to 9. This behavior can be explained in terms of the tetrahedral hydrogen-bonding nature of water. One water molecule can make a maximum of four hydrogen bonds. Therefore, the energy linearly decreases with the coordination numbers from 1 to 4. When the coordination number is 5 or more, the water molecule cannot make hydrogen bonds with all the neighboring water molecules. The excess neighboring water molecules thus prevent the stable tetrahedral hydrogen bonding, and the average energy of one water molecule increases for the coordination numbers from 5 to 9. On the other hand, in the bulk LJ fluid, the average energy has no minimum and linearly decreases as the coordination number increases, because the LJ potential is isotropic. The average energy for each coordination number clearly expresses the characteristics of both water and the LJ fluid.

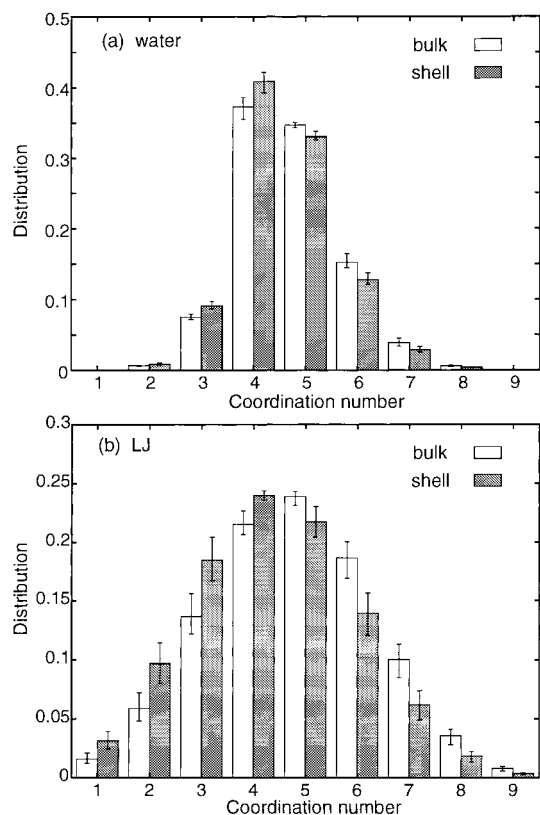


Figure 5. Distribution of the coordination number of (a) water and (b) the Lennard-Jones fluid. Distribution in the bulk molecules is compared with that in the shell molecules around a cavity with λ of 2.5 Å.

We also calculated the average energies of shell molecules around a cavity with λ of 2.5 Å as well as those of bulk molecules. However, the difference between the values for the bulk and the shell was small and almost within the statistical uncertainty, particularly for water (Figure 4a). Therefore, ΔE_{shell} is not due to the average energy change for each coordination number but rather to the distribution change of each coordination number. Figure 5 shows the distribution of each coordination number, $D(c_n)$, in bulk and shell molecules around a cavity with λ of 2.5 Å. The distribution of the LJ fluid is broader than that of water, because the volume fluctuation in the LJ fluid is larger. In Figure 5a, shell water molecules have a larger distribution of coordination numbers that are 4 or less and a smaller distribution of coordination numbers of 5 or more compared to the bulk water molecules. Our results are qualitatively similar to those of Okazaki et al.^{28,29} and Chau et al.,⁴² although they used different intermolecular potentials. In addition, we compared the distribution change of the LJ fluid with that of water. The distribution change of the LJ fluid shows a trend similar to that of water. The distribution change occurs because of the geometrical restriction and is not a special feature of water. If a liquid has the same molecular size and the same density as water, the liquid will show a similar trend in the distribution change.

Combining the average energy with the distribution of the coordination number, we can obtain the energy change for each coordination number $\Delta E_{\text{shell}}^c(c_n)$. The summation of $\Delta E_{\text{shell}}^c(c_n)$ is ΔE_{shell} as follows

$$\Delta E_{\text{shell}}^c(c_n) = \{e_{\text{ave}}^{\text{shell}}(c_n) D^{\text{shell}}(c_n) - e_{\text{ave}}^{\text{bulk}}(c_n) D^{\text{bulk}}(c_n)\} n_{\text{shell}} \quad (5)$$

$$\Delta E_{\text{shell}} = \sum_{c_n} \Delta E_{\text{shell}}^c(c_n) \quad (6)$$

where n_{shell} is the number of water molecules in the hydration shell. For example, n_{shell} is 20 for a cavity with λ of 2.5 Å in water. In eq 5, $e_{\text{ave}}^{\text{shell}}(c_n)$ and $e_{\text{ave}}^{\text{bulk}}(c_n)$ are the average energies of one molecule with the coordination number c_n in, respectively, the shell and the bulk, as shown in Figure 4. $D^{\text{shell}}(c_n)$ and $D^{\text{bulk}}(c_n)$, respectively, are distributions of the coordination number c_n in the shell and the bulk, as shown in Figure 5. Figure 6 shows $\Delta E_{\text{shell}}^c(c_n)$ for water and the LJ fluid. In both cases, $\Delta E_{\text{shell}}^c(c_n)$ for a coordination number of 4 or less is negative and $\Delta E_{\text{shell}}^c(c_n)$ for 5 or more is positive. That is because the distribution of coordination numbers of four or less increases, and the distribution for five or more decreases, upon the change of the molecular state from bulk to shell, as shown in Figure 5. Table 1 shows the summations of $\Delta E_{\text{shell}}^c(c_n)$ for c_n from 1 to 4 ($\Delta E_{\text{shell}}^{1-4}$) and from 5 to 9 ($\Delta E_{\text{shell}}^{5-9}$). In water, $\Delta E_{\text{shell}}^{1-4}$ is balanced with $\Delta E_{\text{shell}}^{5-9}$. In the LJ fluid, $|\Delta E_{\text{shell}}^{5-9}|$ is about double $|\Delta E_{\text{shell}}^{1-4}|$. The reason for this difference is that the average energy for each coordination number has a minimum at 4 or 5 in water but linearly decreases in the LJ fluid as shown in Figure 4.

3.3. Physical Picture of Hydrophobic Hydration at Room Temperature. On the basis of the above results, we can draw a picture of the hydrophobic hydration as follows: When a cavity is formed in the liquid, the coordination number of the molecules around a cavity decreases compared to that of bulk molecules because of the geometrical restriction (the hard-core effect). What occurs upon cavity formation is *not* an energy change for each coordination number *but* a decrease in the coordination number around the cavity. The coordination number of water can decrease with little energy loss at room temperature, because the average energy for each coordination number has a minimum at 4 or 5 in water. In other words, the linear correlation between the coordination number of water and the molecular energy is weak at room temperature because of anisotropic nature of water hydrogen bonding. When a cavity is formed in water, the number of the water configurations that have similar energy levels decreases. This leads to the entropy decrease in hydrophobic hydration at room temperature.

NMR and FT-IR experiments showed that the hydrogen bonds of water around hydrophobic groups are strengthened.¹⁴ This strengthening can be interpreted as a decrease in the coordination number.⁴¹ According to Matubayasi's study,⁴¹ the water geometry can be classified into two types, matching and mismatching. Matching molecules have strong hydrogen bonds, and mismatching molecules do not. In terms of the coordination number, matching geometry corresponds to a coordination number of 4 or less, and mismatching geometry corresponds to a coordination number of 5 or more. The decrease of the number of molecules with a coordination number of 5 or more means a decrease in the mismatching geometry, which leads to the strengthening of hydrogen bonds around hydrophobic groups.

From the point of view of dynamics, some experiments have revealed that water around hydrophobic groups becomes slower.⁵⁷ This decreased mobility can also be interpreted in terms of the coordination number.^{58,59} Through a molecular dynamics simulation, Sciortino et al. showed that molecules with five neighbors diffuse faster than four-coordinated molecules.⁵⁹ Therefore, the water around hydrophobic groups would become slower as a result of the lower coordination number.

3.4. Heat Capacity Change of Hydrophobic Hydration. The change in heat capacity is one of the most important

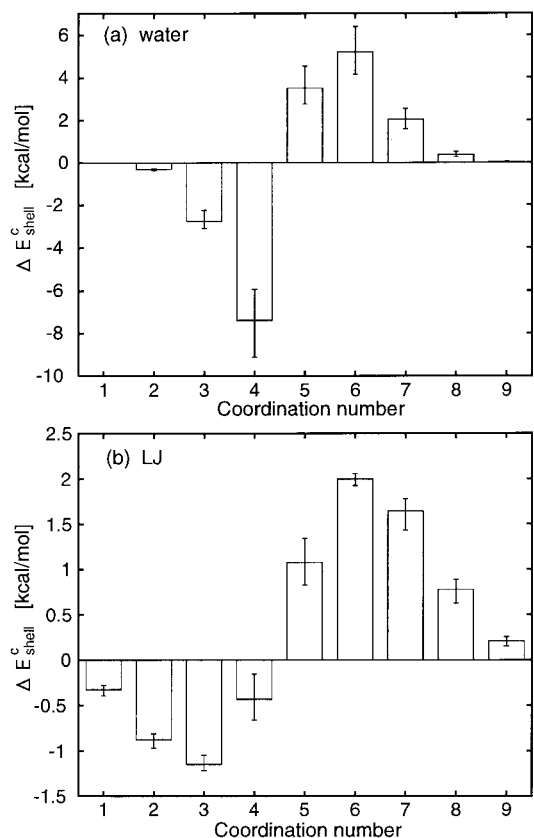


Figure 6. Contribution of each coordination number to ΔE_{shell} in (a) water and (b) the Lennard-Jones fluid.

TABLE 1: ΔE_{shell} of Water and of the Lennard-Jones Fluids for the Coordination Numbers 1–4 and for 5–9

| | $\Delta E_{\text{shell}}^{1-4}$ | $\Delta E_{\text{shell}}^{5-9}$ | $\Delta E_{\text{shell}}^{\text{total}}$ |
|----------|--|---------------------------------|--|
| water | -10.46 ^a (45% → 51%) ^b | 11.18 (55% → 49%) | 0.72 |
| LJ fluid | -2.83 (43% → 56%) | 5.74 (57% → 44%) | 2.91 |

^a The unit of the energy is kcal/mol. ^b The ratio change of distribution (bulk → shell) of the coordination numbers from the bulk state to the shell around a cavity with λ of 2.5 Å.

characteristics of hydrophobic hydration. We applied the coordination number approach in our analysis of the heat capacity change during cavity formation.

Heat capacity is a temperature derivative of enthalpy. Two simulations at slightly different temperatures allow us to calculate the temperature derivatives of properties theoretically, but because of statistical uncertainty, it is difficult to obtain significant values. In this paper, therefore, we chose a high temperature of 363 K (90 °C) for the simulation, so that the thermodynamic properties could be clearly distinguished from those at room temperature.

Figure 7 shows ΔG and ΔE_{shell} at 363 K. At 363 K, ΔG is slightly larger than at 300 K, but ΔE_{shell} at 363 K is significantly larger than at 300 K. The change of ΔE_{shell} can be considered an indicator of the large heat-capacity increment of hydrophobic hydration. Figure 8 shows the average energy for each coordination number at 363 K. The minimum again occurs at the coordination number 5, but the difference in the energy between 4 and 5 (1.5 kcal/mol) is larger than that (0.08 kcal/mol) at 300 K. This means that the coordination number 4 has become less stable. Figure 9 shows the distribution of each coordination number. The changes in the distributions from bulk to shell, that is, the increase for coordination number 4 or less and the decrease for 5 or more, are qualitatively similar to

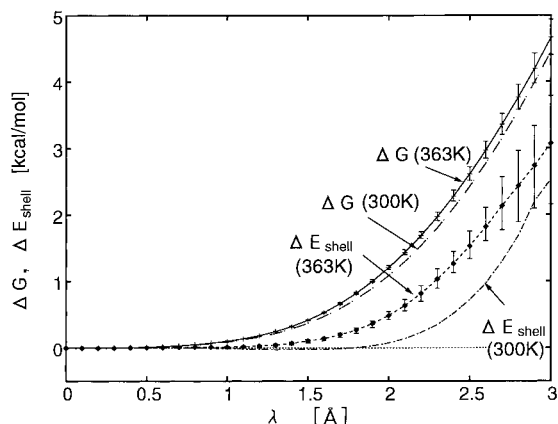


Figure 7. Free energy ΔG and energy change ΔE_{shell} in the hydration shell upon cavity formation in water at 363 K. The values are compared with those at 300 K.

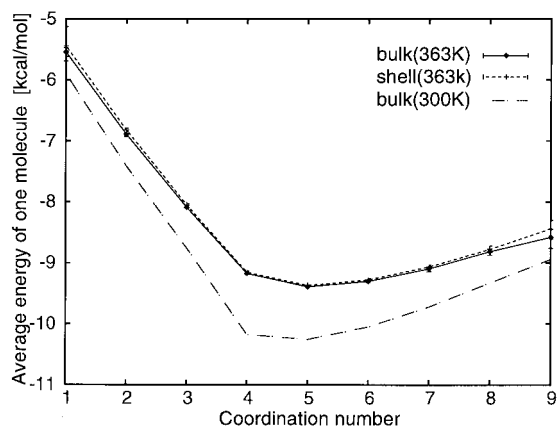


Figure 8. Average energy of one water molecule against the coordination number of the water molecule at 363 K. The energies of the bulk molecules are compared with those of the shell molecules around a cavity with λ of 2.5 Å. The average energy of one bulk molecule at 300 K is also plotted for comparison.

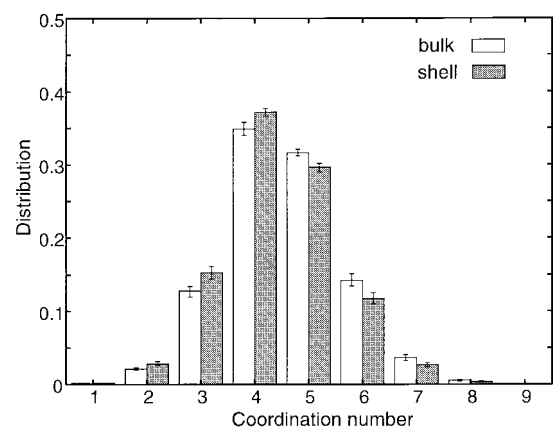


Figure 9. Distribution of the coordination numbers of water at 363 K. The distribution in the bulk molecules is compared with that in the shell molecules around a cavity with λ of 2.5 Å.

those at 300 K. However, the distribution change for the coordination number 4 was smaller than at 300 K.

We also calculated $\Delta E_{\text{shell}}^c(c_n)$ from eq 5 at 363 K and compared it with the value at 300 K. Figure 10 shows $\Delta E_{\text{shell}}^c(c_n)$, and we can see that most of $\Delta E_{\text{shell}}^{363\text{K}} - \Delta E_{\text{shell}}^{300\text{K}}$ is due to $\Delta E_{\text{shell}}^c(c_n)$ for the coordination number c_n of 4. The coordination number of ice is 4, so the increment of $\Delta E_{\text{shell}}^c(4)$ reminds us of the melting of ice. From these results, we

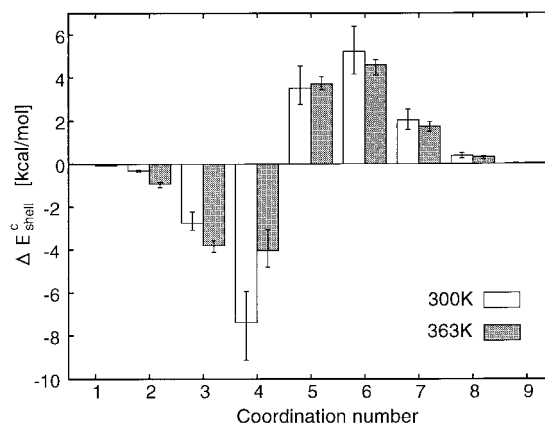


Figure 10. Contribution of each coordination number to ΔE_{shell} in water at 300 K and at 363 K.

developed an understanding of the heat capacity change in hydrophobic hydration that goes as follows: When a water molecule changes its state from bulk to shell, its coordination number changes from 5 or more to 4 or less because of the geometrical restriction. When the coordination number changes to 4, the energy becomes more stable or, at least, does not become unstable. When the coordination number changes to 3 or less, the energy increases. At room temperature, the change to 4 energetically balances with the change to 3 or less. At higher temperatures, the coordination number 4 is less stable, and the ratio of the change to the coordination number 4 becomes smaller than at room temperature. Then ΔE_{shell} increases. In other words, the linear correlation between the coordination number and energy becomes stronger at high temperature than at room temperature. The change of the coordination number to 4, when water molecules change their state from bulk to shell, is considered iceberg formation in terms of the coordination number of water. Thus, the iceberg formation originates from the geometrical restriction of the hard core of molecules and the coordination-number dependence of the energy of water.

3.5. Physical Picture of the Temperature Dependence of Hydrophobic Hydration. To show a clearer unified physical picture of the hydrophobic hydration based on the hydrogen bonding of water and the hard-core effect, we examine the relationship between the temperature dependence of the free energy of cavity formation (related to the hard-core effect) and the energy change near cavities (related to the hydrogen bonding). The enthalpy change ΔH upon cavity formation, which is supposed to be closely related to ΔE_{shell} , is derived from ΔG as follows

$$\Delta H = -kT^2 \left(\frac{\partial \Delta G / kT}{\partial T} \right)_P \quad (7)$$

where the differential is performed under constant pressure. The right-hand side of this equation is divided into a constant-density term and a density-dependent term as follows

$$\Delta H = -kT^2 \left(\frac{\partial \Delta G / kT}{\partial T} \right)_\rho - kT^2 \left(\frac{\partial \Delta G / kT}{\partial \rho} \right)_T \left(\frac{\partial \rho}{\partial T} \right)_P \quad (8)$$

where ρ is the density of the fluids. To estimate the contributions of the first and second terms on the right-hand side of eq 8 to ΔH , the density dependences of $\Delta G/kT$ at 300 and 363 K are shown in Figure 11. For a given density, $\Delta G/kT$ at 363 K differs only slightly from $\Delta G/kT$ at 300 K. Thus, $((\partial \Delta G / kT) / \partial T)_\rho$ is expected to be positive and small, which means that the

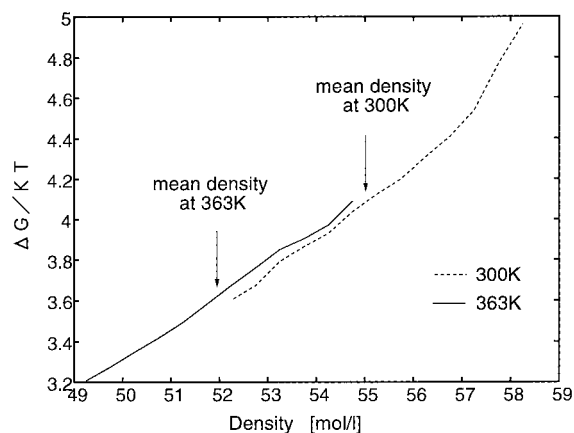


Figure 11. Free energies of cavity formation for various densities at 363 and 300 K.

first term on the right-hand side of eq 8 is negative and small. In Figure 11 it is evident that the slope $((\partial\Delta G/kT)/\partial\rho)_T$ has little dependence on density and temperature. Thus, the remarkable temperature dependence of hydrophobic ΔH is mainly due to the term $(\partial\rho/\partial T)_P$. The term $(\partial\rho/\partial T)_P$ for water is zero at 4 °C (at which water has the maximum density) and decreases rapidly as temperature increases. This is the reason that ΔH is small at room temperature and becomes large at high temperature. Lee²² and Soda,²³ reasoning on the basis of SPT, also pointed out that the term $(\partial\rho/\partial T)_P$ makes the leading contribution to the temperature dependence of ΔH . In SPT, the first term is exactly zero, because SPT is a theory for hard spheres. It is emphasized that our conclusion that the leading contribution to the temperature dependence of ΔH is from $(\partial\rho/\partial T)_P$ is not based on a hard-sphere theory but on the more realistic potential of water.

We then examine the relationship between $(\partial\rho/\partial T)_P$ and ΔE_{shell} . The term $(\partial\rho/\partial T)_P$ is expressed as the correlation of enthalpy and density as follows

$$\left(\frac{\partial\rho}{\partial T}\right)_P = \frac{1}{kT^2} (\langle H\rho\rangle - \langle H\rangle \langle \rho\rangle) \quad (9)$$

At room temperature, because the absolute value of $(\partial\rho/\partial T)_P$ is small, eq 9 implies that enthalpy is insensitive to perturbation of density. At high temperature, the absolute value of $(\partial\rho/\partial T)_P$ becomes large and thus enthalpy becomes more sensitive to perturbation of density. Soda compared the correlation coefficients of the fluctuations in enthalpy and density of organic liquids and water and pointed out that the correlation coefficients of water are remarkably more temperature dependent than those of organic liquids.⁶⁰ The correlation between water energy and density also explains the temperature dependence of ΔE_{shell} , as discussed in section 3.3. In the vicinity of cavities, the coordination number of water (which can be considered as the local density of water) becomes lower than that of bulk water, but the energy change (ΔE_{shell}) is small at room temperature, because of the weak correlation between the coordination number and molecular energy. At high temperature, the correlation of water energy and the coordination number of water becomes stronger and thus ΔE_{shell} becomes larger. We emphasize that both the temperature dependence of ΔH in the thermodynamic level and that of ΔE_{shell} in the molecular level can be explained from the same viewpoint: the temperature dependence of the correlation between energy and density. And, the temperature dependence of the correlation is due to the anisotropic nature of the hydrogen bonding of water, as seen in sections 3.2 and 3.4.

It is necessary to note that our analysis is limited to small cavities, and our conclusion may not apply to larger cavities. We can nonetheless discuss the relation between our results and the insights obtained from previously reported publications concerning water near large cavities or a planar wall. Computer simulations^{61,62} and integral equation studies^{63–65} indicate that water molecules close to large cavities or a planar wall form the “icelike” structure and that water–density profiles near large cavities are characterized as the significant “dewetting” (the decrease of local density). When an idealized icelike structure^{61,62,64} is in contact with a surface, water forms two layers separated from each other by about 0.5 Å. Water molecules in the first layer have the coordination number 3, and water molecules in the second layer have the coordination number 4. This is consistent with our result, which is that the number of 4-or-less coordinated molecules increases around small cavities. Water molecules in the two idealized layers form normal hydrogen bonds to the neighbor molecules. Hydrogen bonds of many (e.g., 6 or more) coordinated molecules near surfaces may be strained. Considering the dewetting at surfaces, however, we expect probability of molecules with such high coordination numbers to be very small.

4. Conclusion

In this paper, the free energy and the energy change of cavity formation in water and in an LJ fluid whose size and density are the same as those of water were calculated using the test particle approach. Our understanding of the effect of the hydrogen bonds and the hard core of molecules on the hydrophobic hydration can be summarized as follows:

(1) The free energy of cavity formation in water at a given density is mainly determined by the hard-core effect.

(2) The leading contribution to the temperature dependence of ΔH of cavity formation is from the temperature dependence of density; that is, from the correlation of enthalpy and density.

(2.1) At room temperature, the small ΔH is due to the weak correlation between enthalpy and density.

(2.2) At high temperatures, the large ΔH is due to the stronger correlation between enthalpy and density.

(3) Near cavities, the coordination number of water (which can be considered as the local density of water) becomes lower than the coordination number of bulk water because of the hard-core effect.

(4) The effect of the hydrogen bonding of water can be seen in the coordination-number dependence of the average energy of one molecule, regardless of whether water is in bulk or in the hydration shell.

(5) Combining the water-specific coordination-number dependence of molecular energy with the decreased coordination number around cavities explains the temperature dependence of the energy change ΔE_{shell} near cavities.

(5.1) At room temperature, the energy change near cavities (ΔE_{shell}) is small because the coordination number can decrease with little energy loss. The correlation between the energy and the coordination number (local density) of water is weak.

(5.2) At high temperatures, the decreased stability of 4-coordinated water caused the stronger correlation between the energy and the coordination number (local density) of water. And then the energy change near cavities (ΔE_{shell}) becomes large.

(6) Both the temperature dependence of ΔH in the thermodynamic level and that of ΔE_{shell} in the molecular level can be explained from the same viewpoint: the temperature dependence of the correlation between energy and density.

(7) The correlation between energy and density is determined by hydrogen bonding of water. This is the major role that the hydrogen bonding of water plays in hydrophobic hydration.

Coordination-number analysis is a simple but powerful way to examine the hydrophobic-hydration mechanism because the coordination number provides a link between the density of liquid and the energetics. In the future, adding some parameters of the hydrogen bonds of water will extend our method to the solvation of polar groups, and this will provide an analysis method for various solvation phenomena, such as protein folding.

Acknowledgment. We thank Prof. K. Soda, Prof. M. Kinoshita, Dr. M. Irisa, Dr. B. Madan, and Dr. P.-L. Chau for their very helpful discussions.

References and Notes

- Ben-Naim, A. *Solvation thermodynamics*; Plenum: New York, 1987.
- Ben-Naim, A. *Statistical Thermodynamics for Chemists and Biochemists*; Plenum: New York, 1992.
- Eisenberg, D.; McLachlan, A. D. *Nature* **1986**, *319*, 119.
- Ooi, T.; Oobatake, M.; Nemethy, G.; Sheraga, H. A. *Proc. Natl. Acad. Sci. U.S.A.* **1987**, *84*, 3086.
- Soda, K.; Hirashima, H. *J. Phys. Soc. Jpn.* **1990**, *59*, 4177.
- Hirashima, H.; Soda, K. *J. Phys. Soc. Jpn.* **1991**, *59*, 330.
- Hirashima, H.; Soda, K. *J. Phys. Soc. Jpn.* **1991**, *60*, 2783.
- Soda, K.; Hirashima, H. *J. Phys. Soc. Jpn.* **1992**, *61*, 2992.
- Shimizu, S.; Ikeguchi, M.; Shimizu, K. *Chem. Phys. Lett.* **1997**, *268*, 93.
- Shimizu, S.; Ikeguchi, M.; Shimizu, K. *Chem. Phys. Lett.* **1998**, *282*, 79.
- Shimizu, S.; Ikeguchi, M.; Nakamura, S.; Shimizu, K. *Chem. Phys. Lett.* **1998**, *284*, 235.
- Privalov, P. L.; Gill, S. J. *Adv. Protein Chem.* **1988**, *39*, 191.
- Frank, H. S.; Evans, M. E. *J. Chem. Phys.* **1945**, *13*, 507.
- Mizuno, K.; Miyashita, Y.; Shindo, Y.; Ogawa, H. *J. Phys. Chem.* **1995**, *99*, 3225.
- Madan, B.; Sharp, K. *J. Phys. Chem.* **1996**, *100*, 7713.
- Sharp, K.; Madan, B. *J. Phys. Chem. B* **1997**, *101*, 4343.
- Shinoda, K. *J. Phys. Chem.* **1977**, *81*, 1300.
- Murphy, K. P.; Privalov, P. L.; Gill, S. J. *Science* **1990**, *247*, 559.
- Pierotti, R. A. *J. Phys. Chem.* **1963**, *67*, 1840.
- Pierotti, R. A. *J. Phys. Chem.* **1965**, *69*, 281.
- Pierotti, R. A. *Chem. Rev.* **1975**, *76*, 717.
- Lee, B. *Biopolymers*. **1985**, *24*, 813.
- Soda, K. *J. Phys. Soc. Jpn.* **1993**, *62*, 1782.
- Lee, B. *Biophys. Chem.* **1994**, *51*, 271.
- Madan, B.; Lee, B. *Biophys. Chem.* **1994**, *51*, 279.
- Geiger, A.; Rahman, A.; Stillinger, F. H. *J. Chem. Phys.* **1979**, *70*, 263.
- Pangali, C.; Rao, M.; Berne, B. J. *J. Chem. Phys.* **1979**, *71*, 2975.
- Okazaki, S.; Nakanishi, K.; Touhara, H.; Adachi, Y. *J. Chem. Phys.* **1979**, *71*, 2421. Erratum: *J. Chem. Phys.* **1980**, *72*, 4253–4254.
- Okazaki, S.; Nakanishi, K.; Touhara, H.; Adachi, Y. *J. Chem. Phys.* **1981**, *74*, 5863.
- J. P. M. Postma, H. J. C. B.; Haak, J. R. *Faraday Symp. Chem. Soc.* **1982**, *17*, 55.
- Rosicky, P. J.; Zichi, D. A. *Faraday Symp. Chem. Soc.* **1982**, *17*, 69.
- Ravishanker, G.; Mezei, M.; Beveridge, D. L. *Faraday Symp. Chem. Soc.* **1982**, *17*, 79.
- Jorgensen, W. L. *J. Chem. Phys.* **1982**, *77*, 5757.
- Rosenberg, R. O.; Mikkilineni, R.; Berne, B. J. *J. Am. Chem. Soc.* **1982**, *104*, 7647.
- Zichi, D. A.; Rosicky, P. J. *J. Chem. Phys.* **1985**, *83*, 797.
- Smith, D. E.; Haymet, A. D. J. *J. Chem. Phys.* **1993**, *98*, 6445.
- Pohorille, A.; Pratt, L. R. *J. Am. Chem. Soc.* **1990**, *112*, 5066.
- Pratt, L. R.; Pohorille, A. *Proc. Natl. Acad. Sci. U.S.A.* **1992**, *89*, 2995.
- Lazaridis, T.; Paulaitis, M. E. *J. Phys. Chem.* **1992**, *96*, 3847.
- Lazaridis, T.; Paulaitis, M. E. *J. Phys. Chem.* **1994**, *98*, 635.
- Matubayasi, N. *J. Am. Chem. Soc.* **1994**, *116*, 1450.
- Chau, P. L.; Forester, T. R.; Smith, W. *Mol. Phys.* **1996**, *89*, 1033.
- Pratt, L. R.; Chandler, D. *J. Chem. Phys.* **1977**, *67*, 3638.
- Pratt, L. R.; Chandler, D. *J. Chem. Phys.* **1980**, *73*, 3430.
- Pratt, L. R.; Chandler, D. *J. Chem. Phys.* **1980**, *73*, 3434.
- Tani, A. *Mol. Phys.* **1983**, *48*, 1229.
- Tani, A. *Chem. Phys. Lett.* **1984**, *105*, 72.
- Ichiye, T.; Chandler, D. *J. Phys. Chem.* **1988**, *92*, 5257.
- Soda, K. *J. Phys. Soc. Jpn.* **1989**, *58*, 4643.
- Soda, K. *J. Phys. Soc. Jpn.* **1990**, *59*, 1093.
- Lue, L.; Blankschtein, D. *J. Phys. Chem.* **1992**, *96*, 8582.
- Ikeguchi, M.; Doi, J. *J. Chem. Phys.* **1995**, *102*, 5011.
- Guillot, B.; Guissani, Y.; Bratos, S. *J. Chem. Phys.* **1991**, *95*, 3643.
- Guillot, B.; Guissani, Y. *J. Chem. Phys.* **1993**, *99*, 8075.
- Matubayasi, N.; Reed, L. H.; Levy, R. M. *J. Phys. Chem.* **1994**, *98*, 10640.
- Jorgensen, W. L.; Chandrasekhar, J.; Madura, J. D.; Impey, R. W.; Klein, M. L. *J. Chem. Phys.* **1983**, *79*, 926.
- Haselmeier, R.; Holz, M.; Marbach, W.; Weingartner, H. *J. Phys. Chem.* **1995**, *99*, 2243.
- Sciortino, F.; Geiger, A.; Stanley, H. E. *Phys. Rev. Lett.* **1990**, *65*, 3452.
- Sciortino, F.; Geiger, A.; Stanley, H. E. *J. Chem. Phys.* **1992**, *96*, 3857.
- Soda, K. *J. Phys. Soc. Jpn.* **1988**, *57*, 4048.
- Lee, C. Y.; McCammon, J. A.; Rosicky, P. J. *J. Chem. Phys.* **1984**, *80*, 4448.
- Valleau, J. P.; Gardner, A. A. *J. Chem. Phys.* **1987**, *86*, 4162.
- Kinoshita, M.; Hirata, F. *J. Chem. Phys.* **1996**, *104*, 8807.
- Vossen, M.; Forstmann, F. *J. Chem. Phys.* **1994**, *101*, 2379.
- Torrie, G. M.; Kusalik, P. G.; Patay, G. N. *J. Chem. Phys.* **1988**, *88*, 7826.